Stanislav Sysala; Jaroslav Haslinger; Sergey Repin

Reliable computation and local mesh adaptivity in limit analysis

In: Jan Chleboun and Pavel Kůs and Petr Přikryl and Miroslav Rozložník and Karel Segeth and Jakub Šístek and Tomáš Vejchodský (eds.): Programs and Algorithms of Numerical Mathematics, Proceedings of Seminar. Hejnice, June 24-29, 2018. Institute of Mathematics CAS, Prague, 2019. pp. 149–158.

Persistent URL: http://dml.cz/dmlcz/703077

Programs and Algorithms of Numerical Mathematics 19
J. Chleboun, P. Kůs, P. Přikryl, M. Rozložník, K. Segeth, J. Šístek, T. Vejchodský (Eds.)
Institute of Mathematics CAS, Prague 2019

RELIABLE COMPUTATION AND LOCAL MESH ADAPTIVITY IN LIMIT ANALYSIS

Stanislav Sysala[1], Jaroslav Haslinger[1], Sergey Repin[2,3]

[1] Institute of Geonics of the Czech Academy of Sciences
Studentská 1768, 708 00 Ostrava, Czech Republic
stanislav.sysala@ugn.cas.cz, hasling@karlin.mff.cuni.cz
[2] University of Jyväskylä
Agora, Mattilanniemi 2, FI-40100 Jyväskylä, Finland
sergey.s.repin@jyu.fi
[3] Peter the Greate St. Petersburg Polytechnic University,
Institute of Applied Mathematics and Mechanics
29 Polytechnicheskaya st., St. Petersburg 195251, Russia

Abstract: The contribution is devoted to computations of the limit load for a perfectly plastic model with the von Mises yield criterion. The limit factor of a prescribed load is defined by a specific variational problem, the so-called limit analysis problem. This problem is solved in terms of deformation fields by a penalization, the finite element and the semismooth Newton methods. From the numerical solution, we derive a guaranteed upper bound of the limit factor. To achieve more accurate results, a local mesh adaptivity is used.

Keywords: limit analysis, von Mises yield criterion, penalization, finite element method, Newton-like method, local mesh adaptivity

MSC: 49M15, 74C05, 74S05, 90C25

1. Introduction

Limit analysis is a rigorous method developed for determination of a limit load applied on a body. This means to find a limit value of a scalar multiplier of a prescribed set of external forces. The presence of the limit load is a feature of perfectly plastic problems. Its knowledge or at least bounds are important since the body collapses beyond this ultimate load. The limit analysis method can be based on a specific variational problem which defines the limit load factor directly without any incremental procedure. This approach is analyzed, e.g., in [4], [15].

The present paper is focused on the limit analysis problem for the von Mises yield criterion and follows on the recent article [9] where computable majorants of the limit load have been investigated. Our aim is to improve numerical results from [9] by using local mesh adaptivity.

DOI: 10.21136/panm.2018.16

The paper is organized as follows. Section 2 is devoted to setting of the limit analysis problem for the von Mises yield criterion. Section 3 deals with a numerical solution of the limit analysis problem involving local mesh adaptivity. In Section 4, we show how to get a computable majorant of the limit load using a posteriori analysis. Section 5 is devoted to an illustrative numerical example. Section 6 concludes the paper with several remarks.

2. Limit analysis problem

In this section, we first present static and kinematic approaches to limit analysis. Then we specify the kinematic limit analysis problem for the von Mises yield criterion.

Let Ω be a bounded domain in $\mathbb{R}^d$, $d = 2, 3$, with the Lipschitz continuous boundary $\partial\Omega$ and Γ_D, Γ_f be open parts of $\partial\Omega$ such that

$$\mathrm{meas}_{d-1}\Gamma_D > 0, \quad \Gamma_D \cap \Gamma_f = \emptyset, \quad \bar{\Gamma}_D \cup \bar{\Gamma}_f = \partial\Omega.$$

We assume that the body is fixed on Γ_D and consider the following space of deformation fields:

$$\mathbb{V} := \{v \in W^{1,2}(\Omega;\mathbb{R}^d) \mid v = 0 \ \text{ on } \Gamma_D\}.$$

On Γ_f, surface forces of density $f \in L^2(\Gamma_f;\mathbb{R}^d)$ are prescribed. Volume forces are represented by a function $F \in L^2(\Omega;\mathbb{R}^d)$. The load functional reads as:

$$L(v) := \int_\Omega F \cdot v \,\mathrm{d}x + \int_{\Gamma_f} f \cdot v \,\mathrm{d}s, \quad v \in \mathbb{V}.$$

By $\mathbb{M}^{d\times d}_{sym}$, we denote the space of symmetric $d \times d$ matrices equipped with the scalar product $e\colon \eta := e_{ij}\eta_{ij}$ and the norm $|e|^2 = e : e$. This space will be used for Cauchy stress tensors and infinitesimal small strain tensors, respectively. Admissible stress tensors belong to a closed, convex set $B \subset \mathbb{M}^{d\times d}_{sym}$ which is usually defined by a (plastic) yield criterion. We assume a homogeneous material and thus B does not vary in Ω. The symbol $\varepsilon(v) = (\nabla v + (\nabla v)^\top)/2$ stands for the linearized strain tensor related to $v \in \mathbb{V}$.

The following two sets define statically and plastically admissible stress fields, respectively:

$$Q_{\lambda L} := \left\{\tau \in L^2(\Omega, \mathbb{M}^{d\times d}_{sym}) \mid \int_\Omega \tau : \varepsilon(v) \,\mathrm{d}x = \lambda L(v) \quad \forall v \in \mathbb{V}\right\},$$
$$P := \left\{\tau \in L^2(\Omega, \mathbb{M}^{d\times d}_{sym}) \mid \ \tau(x) \in B \quad \text{for a.a. } x \in \Omega\right\},$$

where $\lambda \geq 0$ is the load parameter (factor). Thus any element belonging to $Q_{\lambda L}$ satisfies the balance equation in Ω and the Neumann boundary conditions on Γ_f with respect to the loads λF and λf, respectively. The static limit value λ^* is defined as the supremum over all λ, for which there exists simultaneously a statically and plastically admissible stress field, i.e.,

$$\lambda^* := \sup\{\lambda \geq 0 \mid \ Q_{\lambda L} \cap P \neq \emptyset\}.$$

The kinematic approach to limit analysis is based on the minimization of the plastic dissipation functional subject to the load constraint:

$$(\mathcal{P})^\infty \qquad \zeta^* := \inf_{\substack{v\in\mathbb{V}\\ L(v)=1}} J_\infty(v), \quad J_\infty(v) := \int_\Omega j_\infty(\varepsilon(v))\,\mathrm{d}x, \quad v \in \mathbb{V},$$

where

$$j_\infty : \mathbb{M}^{d\times d}_{sym} \to \overline{\mathbb{R}}_+, \quad \overline{\mathbb{R}}_+ := \mathbb{R}_+ \cup \{+\infty\}, \quad j_\infty(e) := \sup_{\tau\in B} \tau : e.$$

We see that the function j_∞ need not be finite everywhere and thus one must expect additional constraints in $(\mathcal{P})^\infty$ depending on the definition of B. Further, it is worth noticing that the space $\mathbb{V}$ is sufficient for the definition of the kinematic limit value ζ^* but the minimum of J_∞ need not belong to $\mathbb{V}$, in general. This is due to the fact that the functional J_∞ has only a linear growth at infinity in its effective domain. Therefore, J_∞ is coercive only in the space $W^{1,1}(\Omega,\mathbb{R}^d)$ which is not reflexive. A minimizer can be found in the BD space after a certain relaxation of the problem. This space contains functions with bounded deformations which can be discontinuous along surfaces and it enables us to describe expected failure mechanisms in limit analysis.

The following duality relationship between the static and kinematic approaches holds:

$$\lambda^* = \sup_{\substack{\tau\in L^2(\Omega,\mathbb{M}^{d\times d}_{sym})\\ \tau\in B \text{ in}\Omega}} \inf_{\substack{v\in\mathbb{V}\\ L(v)=1}} \int_\Omega \tau : \varepsilon(v)\,\mathrm{d}x \le \inf_{\substack{v\in\mathbb{V}\\ L(v)=1}} \int_\Omega j_\infty(\varepsilon(v))\,\mathrm{d}x = \zeta^*,$$

i.e., $\lambda^* \le \zeta^*$, in general. However, the equality can be proven for specific B's.

The von Mises yield criterion defines the set B in the form

$$B = \left\{\tau \in \mathbb{M}^{d\times d}_{sym} \mid \ |\tau^D| \le \gamma\right\}, \tag{1}$$

where $\tau^D = \tau - \frac{1}{d}(\operatorname{tr}\tau)I$ is the deviatoric part of τ, $\operatorname{tr}\tau = \tau_{ii}$ is the trace of τ, I is the identity matrix in $\mathbb{M}^{d\times d}_{sym}$, and $\gamma > 0$ represents an initial yield stress. Notice that B is an unbounded cylinder aligned with the hydrostatic axis. For this particular choice of B, one can specify the function j_∞ and consequently the problem $(\mathcal{P})^\infty$. We have:

$$j_\infty(e) = \sup_{\tau\in B} \tau : e = \begin{cases} \gamma|e^D|, & \operatorname{tr} e = 0 \\ +\infty, & \operatorname{tr} e \neq 0 \end{cases} \qquad \forall e \in \mathbb{M}^{d\times d}_{sym},$$

and

$$\zeta^* = \inf_{\substack{w\in\mathbb{S}\\ L(w)=1}} J^M_\infty(w), \qquad J^M_\infty(w) := \int_\Omega \gamma|\varepsilon^D(w)|\,\mathrm{d}x, \tag{2}$$

where

$$\mathbb{S} = \{w \in \mathbb{V} \mid \operatorname{div} w = 0 \text{ a.e. in } \Omega\}.$$

Clearly, (2) is a non-smooth optimization problem involving the isoperimetric and divergence-free constraints. For this model we know that $\lambda^* = \zeta^*$ (see [15]).

3. Numerical solution

Numerical strategy presented below has been developed in [1], [6], [7], [12], [14] and it can be used for various types of the set B, not only for (1). It is based on the following penalization of problem $(\mathcal{P})^\infty$:

$$(\mathcal{P})^\alpha \qquad \inf_{\substack{v\in\mathbb{V},\\ L(v)=1}} \int_\Omega j_\alpha(\varepsilon(v))\,\mathrm{d}x, \quad j_\alpha(e) := \sup_{\tau\in B}\{\tau : e - \frac{1}{2\alpha}\mathbb{C}^{-1}\tau : \tau\}, \quad e\in\mathbb{M}^{d\times d}_{sym},$$

where $\alpha > 0$ is the penalization parameter and $\mathbb{C}$ is a symmetric and positive definite fourth order tensor. Regardless of a particular choice of $\mathbb{C}$, it holds that j_α is convex, smooth, real-valued in $\mathbb{M}^{d\times d}_{sym}$, and $j_\alpha \to j_\infty$ pointwisely as $\alpha \to +\infty$. For example, if B is defined by (1) and $\mathbb{C}$ is the identity tensor then

$$j_\alpha(e) = \begin{cases} \frac{\alpha}{2} e : e, & |e^D| \le \gamma/\alpha \\ \frac{\alpha}{2}\left[e : e - (|e^D| - \gamma/\alpha)^2\right], & |e^D| \ge \gamma/\alpha \end{cases} \qquad \forall e \in \mathbb{M}^{d\times d}_{sym},$$

$$j'_\alpha(e) = \begin{cases} \alpha e, & |e^D| \le \gamma/\alpha \\ \alpha\left[e - (|e^D| - \gamma/\alpha)\frac{e^D}{|e^D|}\right], & |e^D| \ge \gamma/\alpha \end{cases} \qquad \forall e \in \mathbb{M}^{d\times d}_{sym},$$

where $j'_\alpha(e)$ is the Fréchet derivative of j_α at e. Similar formulas can be found, e.g., in [6], [15].

A minimizer of the penalized problem need not belong to $\mathbb{V}$ similarly as for problem $(\mathcal{P})^\infty$. But if we admit that the minimizer belongs to $\mathbb{V}$ and denote it as u_α, then there exists $\lambda_\alpha \ge 0$ such that the pair $(u_\alpha, \lambda_\alpha)$ is a solution to the following problem:

$$\int_\Omega \Pi_B(\varepsilon(\alpha u_\alpha)) : \varepsilon(v)\,\mathrm{d}x = \lambda_\alpha L(v) \ \ \forall v \in \mathbb{V} \quad \text{and} \quad L(u_\alpha) = 1, \tag{3}$$

where $\Pi_B(\alpha e) := j'_\alpha(e)$ for any $\alpha > 0$, $e \in \mathbb{M}^{d\times d}_{sym}$ and Π_B represents the projection of $\mathbb{M}^{d\times d}_{sym}$ onto B. The first equation in (3) is closely related to Hencky's problem for a load parameter λ, see [6], [15]. It is important to note that the mapping $\psi\colon \alpha \mapsto \lambda_\alpha$ is meaningful even if $u_\alpha \notin \mathbb{V}$. Moreover, ψ is a continuous and nondecreasing function in $\mathbb{R}_+$ and $\psi(\alpha) \to \lambda^*$ as $\alpha \to +\infty$, see [7].

Next, the penalized problem is discretized by conforming finite elements belonging to a space $\mathbb{V}_h \subset \mathbb{V}$. The discrete counterparts of $(\mathcal{P})^\alpha$, u_α, ψ, and λ^* are denoted as $(\mathcal{P})^\alpha_h$, $u_{\alpha,h}$, ψ_h, and λ^*_h, respectively. The solution $u_{\alpha,h}$ to $(\mathcal{P})^\alpha_h$ always exists unlike continuous setting of the problem. The function ψ_h can be directly defined as follows:

$$\psi_h(\alpha) := \int_\Omega \Pi_B(\varepsilon(\alpha u_{h,\alpha})) : \varepsilon(u_{h,\alpha})\,\mathrm{d}x, \quad \alpha > 0, \tag{4}$$

It is also a continuous, nondecreasing function in $\mathbb{R}_+$ and $\psi_h(\alpha) \to \lambda^*_h$ as $\alpha \to +\infty$, see [7], [14]. If we consider a regular system of finite element meshes then $\psi_h(\alpha) \to \psi(\alpha)$ as $h \to 0_+$ for any $\alpha > 0$, see [7]. Unfortunately, convergence $\lambda^*_h \to \lambda^*$ may not hold. We only know that $\lambda^*_h \ge \lambda^*$.

The discrete counterpart to (3) is solved by the semismooth Newton method with damping. It leads to a sequential quadratic programming inside problem $(\mathcal{P})_h^\alpha$ and due to the damping, it can be interpreted as a descent direction method. For convergence analysis, we refer to [1]. To find a sufficiently large value of α for which the function ψ_h is already almost constant, we use a continuation technique with respect to α, see also [9], [13].

In limit analysis, the failure is usually localized and rigid deformation fields are observed far from the failure. Therefore, local mesh adaptivity can significantly reduce the number of unknowns and improve accuracy of the results. Our refinement procedure is available only for 2D cases which result from the plane strain reduction of 3D problems. For the sake of simplicity, we consider right-angled and isosceles triangles (elements) before and after the refinement to avoid a mesh degeneration. The refined mesh is constructed by means of the bisection technique.

We use the following mesh adaptive strategy. First, the maximal value $\widehat{\alpha}$ of α achieved by the continuation on the coarsest mesh $\mathcal{T}_{h_0}$ is fixed. For the mesh level $k = 0, 1, 2, \ldots$, we denote the solution to $(\mathcal{P})_{h_k}^{\widehat{\alpha}}$ by u_k. Then $\int_T \gamma|\varepsilon^D(u_k)|\,\mathrm{d}x$ is evaluated for any $T \in \mathcal{T}_{h_k}$ and 10% of elements with the largest integral values is selected. This set of elements is slightly modified to be the $(k+1)$-th mesh level created by right-angled triangles. For $k = 1, 2, \ldots$, problem $(\mathcal{P})_{h_k}^{\widehat{\alpha}}$ is solved by the damped Newton method without continuation. For better convergence, we use u_{k-1} on the finer mesh to initiate Newton's method. Notice that the integrals $\int_T \gamma|\varepsilon^D(u_k)|\,\mathrm{d}x$ correspond to the function J_∞^M introduced in (2). Therefore, this quantity was chosen for the adaptive mesh refinement.

The problem is implemented in Matlab. Tangential stiffness matrices and load vectors are assembled by vectorized codes described in [2]. These codes are available for P1, P2, Q1 and Q2 elements in 2D and 3D. For numerical examples presented below, we use P2 elements with the 7-point Gauss quadrature for numerical integration on triangular elements.

4. Computable majorants of the limit load

Limit analysis was originally developed as an analytical method determining lower and upper bounds of the limit load, see [3], [11] and the references therein. Indeed, from (2), we obtain the following upper bound:

$$\zeta^* \le \frac{J_\infty^M(w)}{L(w)} \quad \forall w \in \mathbb{S},\ L(w) > 0. \tag{5}$$

Unfortunately, this bound holds only for divergence-free functions w and thus it cannot be combined with the numerical solution from Section 3. We sketch an idea how to extend this bound to a broader class of functions which need not satisfy the divergence-free constraint. For more details we refer to [9].

The extension of (5) is based on the following distance estimate between functions from $\mathbb{V}$ and the space $\mathbb{S}$, [8], [9]: for any $v \in \mathbb{V}$ there exists $w \in \mathbb{S}$ such that

$$\|\nabla(v-w)\|_\Omega \le E(\operatorname{div} v) := \|\{\operatorname{div} v\}_\Omega \nabla u_*\|_\Omega + C_\Omega \|\operatorname{div} v - \{\operatorname{div} v\}_\Omega \operatorname{div} u_*\|_\Omega , \quad (6)$$

where $\{g\}_\Omega$ denotes the integral mean value of a function g in Ω, $u_* \in \mathbb{V}$ is an arbitrary function satisfying $\{\operatorname{div} u_*\}_\Omega = 1$ and $C_\Omega > 0$ is a constant depending only on the shape of Ω. The inverse of $C_\Omega > 0$ equals to a lower bound in the well-known inf-sup condition for incompressible flow media:

$$\inf_{\substack{q\in L^2(\Omega)\\ \{q\}_\Omega=0}} \sup_{v\in W_0^{1,2}(\Omega;\mathbb{R}^d)} \frac{\int_\Omega q \operatorname{div} v \,\mathrm{d}x}{\|q\|_\Omega \|\nabla v\|_\Omega} \ge C_\Omega^{-1}.$$

The bound C_Ω is known in the literature for specific simple shaped domains Ω [5]. Otherwise, it is possible to extend (6) by using a domain decomposition of Ω into simpler subdomains [8], [9]. The function u^* can be computed numerically by a minimization of $\|\nabla v\|_\Omega^2$ in $\mathbb{V}_h$ subject to $\{\operatorname{div} v\}_\Omega = 1$.

From (6), two consequences follow for limit analysis: $\lambda^* = \zeta^*$ and the upper bound

$$\zeta^* \le \frac{J_\infty^M(v) + \gamma|\Omega|^{1/2} E(\operatorname{div} v)}{L(v) - \|L\|_+ E(\operatorname{div} v)}, \quad \forall v \in \mathbb{V},\ L(v) > \|L\|_+ E(\operatorname{div} v), \quad (7)$$

where $\|L\|_+$ denotes an upper bound of

$$\|L\|_* := \sup_{\substack{v\in\mathbb{V}\\ v\neq 0}} \frac{|L(v)|}{\|\nabla v\|_\Omega}.$$

Notice that the bound $\|L\|_+$ can be found analytically for the example presented in Section 5. In general, one can derive computable majorants of $\|L\|_*$, see, e.g., [10]. Therefore the bound (7) is computable.

Inserting the solution $u_{h,\alpha}$ of $(\mathcal{P})_h^\alpha$ into (7), we arrive at the following upper bound function:

$$\Psi_h(\alpha) = \begin{cases} \dfrac{J_\infty^M(u_{h,\alpha}) + \gamma|\Omega|^{1/2} E(\operatorname{div} u_{h,\alpha})}{1 - \|L\|_+ E(\operatorname{div} u_{h,\alpha})}, & \text{if } 1 > \|L\|_+ E(\operatorname{div} u_{h,\alpha}), \\ +\infty, & \text{otherwise,} \end{cases} \quad (8)$$

Clearly, $\Psi_h(\alpha) \ge \lambda^*$ for any $\alpha > 0$. Moreover, $\Psi_h(\alpha) \to \lambda_h^*$ as $\alpha \to +\infty$ and $\inf_{\alpha>0} \Psi_h(\alpha) \to \lambda^*$ as $h \to 0_+$, see [9].

5. Numerical example

In this section, we consider a plane strain problem in $\Omega = (0,10)\times(0,10)\setminus[0,1]\times[0,1]$, see Figure 2. On the left and bottom sides of $\partial\Omega$, the symmetric boundary

conditions are prescribed, i.e. $v_1(0, x_2) = 0$ for $x_2 \in (1, 10)$ and $v_2(x_1, 0) = 0$ for $x_1 \in (1, 10)$. The load functional L is defined only by the constant traction of density $f = (0, 450)$ acting on the upper side of $\partial\Omega$, i.e. $L(v) = 450 \int_0^{10} v_2(x_1, 10)\, \mathrm{d}x_1$, $v = (v_1, v_2) \in \mathbb{V}$. We set $\gamma = 450\sqrt{2/3}$. Finally, the analytical bounds $\|L\|_+ \doteq 4640$ and $C_\Omega \doteq 2.9745$ are at our disposal, see [9].

We compare the values $\psi_h(\alpha)$ and $\Psi_h(\alpha)$ computed by the P2 elements for different mesh levels. The resulting curves are depicted in Figure 1. The figure on the left corresponds to the coarsest mesh where the continuation through α was used. We see that the upper bound function Ψ_h is decreasing and thus the values $\Psi_h(\alpha)$ overestimate λ^* for α small. But for the maximal value $\widehat{\alpha} \doteq 10^6$ both curves practically coincide and thus they are close to λ_h^* as follows from the theoretical results. Then the local mesh adaptivity for $\alpha = \widehat{\alpha}$ with 48 mesh levels is used, see the figure on the right. During the mesh refinement, the bounds of λ^* are reduced. We see that the difference between $\psi_h(\widehat{\alpha})$ and $\Psi_h(\widehat{\alpha})$ remains almost constant and $\psi_h(\widehat{\alpha}) \doteq 1.0311$ and $\Psi_h(\widehat{\alpha}) \doteq 1.0313$ for the finest mesh with more than 200 thousands unknowns. The (guaranteed) upper bound 1.0313 is slightly lower than in [9], where we found the value 1.0319 using a very fine regular mesh. Since $\lim_{h\to 0_+} \psi_h(\widehat{\alpha}) = \psi(\widehat{\alpha}) \leq \lambda^*$, one can expect that $\lambda^* \doteq 1.03$ from the trend in the figure on the right.

The finest mesh and its detail are depicted in Figure 2. We see that the mesh was refined only in the central diagonal band of Ω. On the remaining parts of the domain, the original (coarsest) mesh is preserved. It is worth noticing that the diagonal band was not clearly visible within first few mesh levels. From the detail of the finest mesh, one can see that the smallest elements are located in a vicinity of the point $[1, 1]$ and on the boundary of this band.

The finest mesh corresponds to the failure visualized in Figure 3. Here, we depict $|\varepsilon^D(u_{h,\widehat{\alpha}})|$ (left) and $|u_{h,\widehat{\alpha}}|$ (right). One can observe a significant jump of $u_{h,\widehat{\alpha}}$ at the point $[1, 1]$ and rigid deformation at the left-top, right-top and right-bottom triangles, see dark regions in Figure 3 (left). The distribution of $|\varepsilon^D(u_{h,\widehat{\alpha}})|$ is similar but sharper than in [9]. Due to this comparison with the regular mesh, we see that the mesh adaptive strategy was successfull and in accordance with the expected failure.

6. Conclusion

This contribution followed on our recent research from [1], [6], [7], [9], [12], [14], where efficient numerical methods for solving the kinematic limit analysis problem and reliable estimates of the limit load have been developed. Here, we enhanced this concept by a simple local mesh adaptivity and illustrated that it can lead to more accurate results.

Acknowledgements

This work was supported by The Ministry of Education, Youth and Sports of the Czech Republic from the National Programme of Sustainability (NPU II), project "IT4Innovations excellence in science - LQ1602".

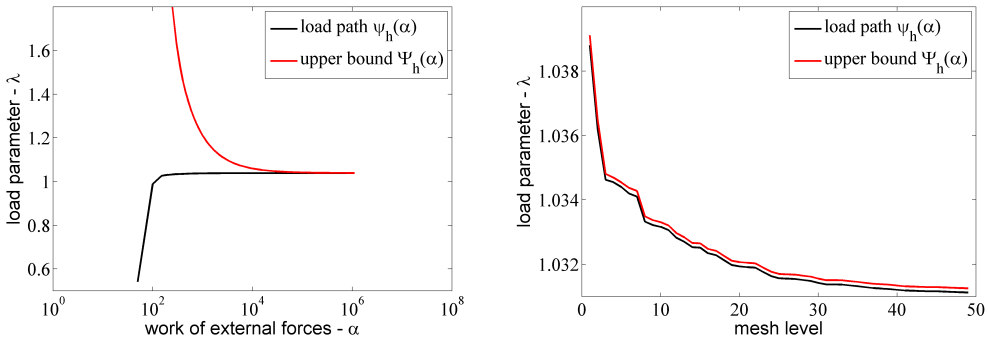

Figure 1: Comparison of $\psi_h(\alpha)$ and $\Psi_h(\alpha)$ on the coarsest mesh (left) and on the different mesh levels for $\alpha = \widehat{\alpha}$ (right).

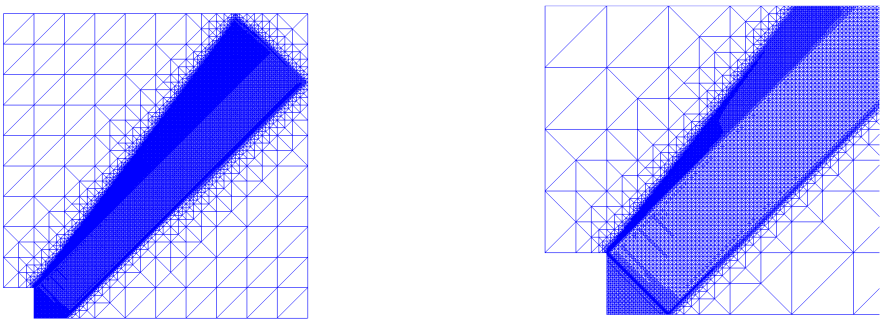

Figure 2: The finest mesh and its detail.

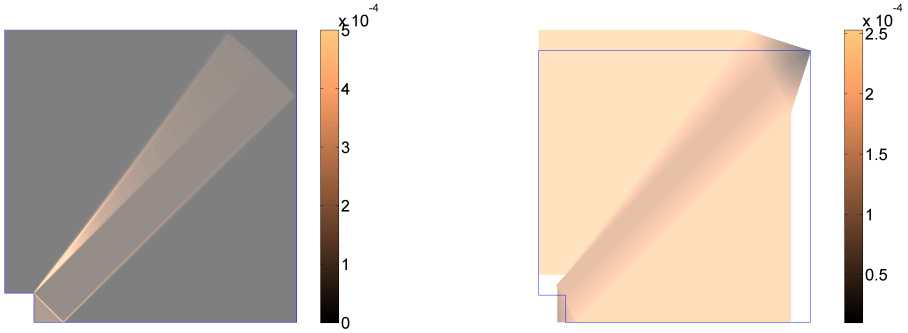

Figure 3: Visualization of the failure by $|\varepsilon^D(u_{h,\widehat{\alpha}})|$ (left) and $|u_{h,\widehat{\alpha}}|$ (right).

References

[1] Cermak, M., Haslinger, J., Kozubek, T., and Sysala, S.: Discretization and numerical realization of contact problems for elastic-perfectly plastic bodies. Part II–numerical realization, limit analysis. ZAMM-Journal of Applied Mathematics and Mechanics/Zeitschrift für Angewandte Mathematik und Mechanik **95** (2015), 1348–1371.

[2] Čermák, M., Sysala, S., and Valdman, J.: Fast matlab assembly of elastoplastic fem matrices in 2d and 3d. arXiv preprint arXiv:1805.04155 (2018).

[3] Chen, W.F. and Liu, X.: *Limit analysis in soil mechanics*, vol. 52. Elsevier, 2012.

[4] Christiansen, E.: Limit analysis of collapse states. In: *Handbook of numerical analysis (P.G. Ciarlet and J.L. Lions eds., Vol IV, Part 2)*. North-Holland, 1996 pp. 193–312.

[5] Costabel, M. and Dauge, M.: On the Inequalities of Babuška–Aziz, Friedrichs and Horgan–Payne. Archive for Rational Mechanics and Analysis **217** (2015), 873–898.

[6] Haslinger, J., Repin, S., and Sysala, S.: Guaranteed and computable bounds of the limit load for variational problems with linear growth energy functionals. Applications of Mathematics **61** (2016), 527–564.

[7] Haslinger, J., Repin, S., and Sysala, S.: A reliable incremental method of computing the limit load in deformation plasticity based on compliance: Continuous and discrete setting. Journal of Computational and Applied Mathematics **303** (2016), 156–170.

[8] Repin, S.: Estimates of the Distance to the Set of Divergence Free Fields. Journal of Mathematical Sciences **210** (2015), 822–834.

[9] Repin, S., Haslinger, J., and Sysala, S.: Computable majorants of the limit load in hencky's plasticity problems. Computer & Mathematics with Applications **75** (2018), 199–217.

[10] Repin, S.I.: *A posteriori estimates for partial differential equations*, vol. 4. Walter de Gruyter, 2008.

[11] Sloan, S.: Geotechnical stability analysis. Géotechnique **63** (2013), 531.

[12] Sysala, S., Haslinger, J., Hlaváček, I., and Cermak, M.: Discretization and numerical realization of contact problems for elastic-perfectly plastic bodies. Part I–discretization, limit analysis. ZAMM-Journal of Applied Mathematics and Mechanics/Zeitschrift für Angewandte Mathematik und Mechanik **95** (2015), 333–353.

[13] Sysala, S., Čermák, M., and Ligurský, T.: Subdifferential-based implicit return-mapping operators in mohr-coulomb plasticity. ZAMM-Journal of Applied Mathematics and Mechanics/Zeitschrift für Angewandte Mathematik und Mechanik **97** (2017), 1502–1523.

[14] Sysala, S. and Haslinger, J.: Truncation and indirect incremental methods in Hencky's perfect plasticity. In: *Mathematical Modelling in Solid Mechanics*, pp. 265–284. Springer series "Advanced Structured Materials", 2017.

[15] Temam, R.: *Mathematical problems in plasticity.* Paris, 1985.